CONFERENCE PRE-PRINT

INVESTIGATING THE FORMATION AND GROWTH OF FUZZY NANO-STRUCTURES DUE TO THE INTERACTION OF HELIUM PLASMA WITH TUNGSTEN UTILIZING A DC GLOW DISCHARGE PLASMA DEVICE

F.Sedighi

Atomic Energy Organization of Iran (AEOI)

Tehran, Islamic Republic of Iran

Email (Corresponding Author): fsedighi@aeoi.org.ir

D.Iraji

Amirkabir University of Technology (AUT)

Tehran, Islamic Republic of Iran

Email (Corresponding Author): iraji@aut.ac.ir

C.Rasouli

Atomic Energy Organization of Iran (AEOI)

Tehran, Islamic Republic of Iran

M.B.Mahmoudi

Atomic Energy Organization of Iran (AEOI)

Tehran, Islamic Republic of Iran

A.Mazandarani

Atomic Energy Organization of Iran (AEOI)

Tehran, Islamic Republic of Iran

Abstract

Helium glow discharge cleaning is one of the primary methods of tokamak wall conditioning, particularly effective in minimizing hydrogen and deuterium retention, while also reducing impurities such as oxygen and hydrocarbons. Due to the fact that in glow discharge regime the energy of ions is low, the probability of any serious damage to the refractory plasma facing materials, such as tungsten and molybdenum is considered very low. Recent reports about the interaction of low-energy helium ions with tungsten surfaces reveal that these low-energy ions can cause serious and profound damage to tungsten and molybdenum surfaces. For this purpose, a series of experiments have been performed in Damavand tokamak, and also in a DC glow discharge plasma device (a PECVD device) which investigates the microscopic effects of helium glow discharge plasma on tungsten and molybdenum surfaces. The results of these experiments are remarkable. In some areas, the growth and formation of fuzzy nanostructures were observed, which probably have a loose structure and can be easily detached from the surfaces and lead to contamination. Morphological changes have also occurred in some areas. The results of XRD analysis show that the peak positions are shifted slightly. The amount of the shifts in XRD peaks increases with increasing helium ion fluence. However, no new peak has been observed which means no new phase has been created in the structure by the irradiation. The results show that although helium glow discharge cleaning is a routine and useful method for stainless steel vacuum vessel conditioning, it may have some side effects for refractory materials such as tungsten and molybdenum.

1. INTRODUCTION

As fusion research advances toward long-pulse and steady-state tokamak operations, the degradation of plasmafacing materials remains a critical challenge. Actually, Plasma-material interactions play a critical role in determining the performance and longevity of plasma-facing components in fusion devices. Among various plasma species, helium has a unique effect on materials, particularly tungsten, which is widely used in tokamak divertors due to its high melting point, low sputtering yield, and excellent thermal conductivity. However, prolonged helium plasma exposure can lead to significant surface modifications, including the formation of helium bubbles, nanostructures, and fibre-like "fuzzy" growths, which can alter the material's properties. Understanding these effects is crucial for predicting material behaviour in future fusion reactors and optimizing plasma-facing components for long-term operation.

A high quality plasma with the least amount of impurities is one the most important features in tokamaks. Various factors cause the quality of plasma to decrease, in which the plasma-wall interaction plays a decisive role. The interaction of energetic ions with the walls of chamber causes to release of several low-Z and high-Z impurities into the plasma. The presence of impurities could have harmful effects on plasma evolution. For example, the bremsstrahlung radiation leads to cool plasma, and eventually loss of the plasma [1]. The other important harmful effect of impurities is the dilution of plasma which reduces the fusion power. On the other hand, the plasma particles could be trapped inside the wall, which can be released from the wall again over time and enter the plasma environment, which also reduces the quality of plasma and control of plasma density. Therefore, wall conditioning has a key role to remove impurities and improve plasma quality. There are several wall conditioning methods such as baking, thin film deposition, ion cyclotron resonance, and glow discharge cleaning (GDC) which among these methods, GDC is of considerable importance [2-6].

Glow discharge is a type of plasma created by passing an electric current through a gas. It is formed by applying voltage between two electrodes in a vacuum vessel containing a low-pressure gas. The glow discharge regime is commonly used in tokamaks and one of its most important applications is vacuum vessel wall conditioning [6, 7]. In the process of GDC, various gases such as hydrogen, helium, neon, and argon are used, each of which has its own characteristics and advantages. Helium glow discharge cleaning is an important process that is commonly used to reduce impurities such as oxygen from the vacuum vessel. Since ions have low energy in the GDC regime, the possibility of serious damage to the plasma-facing components (PFCs), which are often from hard and resistant materials, by them is unlikely. For this reason, there are few reports about the interaction of ions in GDC regime with PFCs. However, in a series of studies performed to GDC in LHD stellarator, microscopic damage of materials has been reported [8-10]. Nevertheless, the GDC method is currently considered as one of the most important wall conditioning methods in current tokamaks and future ITER reactor [11-14].

The materials used to construct the Plasma facing components have to operate over the lifetime of a fusion reactor vacuum vessel by handling the harsh environmental conditions, such as ion bombardment causing physical and chemical sputtering and therefore erosion, ion implantation causing displacement damage and chemical composition changes, and high heat fluxes about 10MW/m² due to ELMS instability. Therefore, tungsten (W) due to its outstanding properties such as high melting point, low sputter erosion, and low activation has always been one of the main PFC candidates. In addition to W, molybdenum (Mo) has always been mentioned as a suitable alternative to tungsten. Interaction of plasma ions with the tokamak wall has always been one of the most challenging issues for constructing a fusion reactor. Although it has long been thought that low-energy ions (below 200eV) could not cause any considerable damage to plasma-facing materials (PFMs), reports in recent years about the interaction of low-energy ions with refractory materials such as W and Mo have raised concerns. The reports show that low-energy helium ions can cause serious changes in the tungsten and molybdenum surfaces [15-17]. For example, Wright et al. showed that interaction of lowenergy helium ions ($T_e \approx 25 eV$) with tungsten in divertor region of Alcator C-Mod tokamak can cause changes in tungsten surface, as well as the formation and growth of nanostructures that can be easily separated from the surface. These loose nanostructures could be a source of dust particles and impurities which leads to cool plasma [18, 19].

Due to the importance of the interaction of low-energy ions with PFMs, extensive research has been conducted in recent years with various devices to investigate this issue in more detail [19-22]. Since helium ions have low energy in He-GDC procedure, and on the other hand, considering that He-GDC is one of the most important wall conditioning methods in current tokamaks and future ITER reactor, it was decided to investigate the microscopic effects of helium glow discharge on W and Mo specimens as the main PFM candidates. The results obtained in Damavand tokamak and also in a PECVD device are interesting and can provide useful information on the effect of He-GDC method on the tungsten and molybdenum.

2. EXPERIMENTAL DETAILS

The experiments have been conducted in Damavand tokamak and a PECVD device. The materials used are pure (99.9%) W sheets (0.1mm thick), and pure (99.5%) Mo sheets (0.2mm thick) cut in 10×20mm2. These specimens were mechanically polished to a mirror-like surface finish. After that, each sample was installed on material probe which was electrically connected to the vacuum vessel. The probe is actually a dual-purpose probe which, in addition to being used as a Langmuir probe, can also be used as a material probe. The schematic of the experiment is shown in Fig. 1 and Fig.2. The glow discharge electrodes consist of stainless steel (SS) rods, each 10 cm in length and 1 cm in diameter. They are inserted through a lower port using insulators and positioned within the large section of the vacuum chamber at two cross-sections. A positive potential is applied

to the electrodes relative to the chamber wall. Following exposure to atmospheric conditions, the system typically requires 5–7 days to reach stable operating conditions. The glow discharge parameters such as electron temperature, ion density, and plasma potential measured by Langmuir probe are 6eV, $1.2\times10^{15} \text{m}^{-3}$, and 240V respectively. The calculated ion flux is about 2.4×10^{18} ions/s¹m² and the helium ions energy impacted to the surface is 240 eV. The residual gas analysis (RGA) data during the GDC process were not available in the present study. Future work should aim to incorporate in-situ RGA measurements to better quantify impurity levels and plasma-surface interactions.

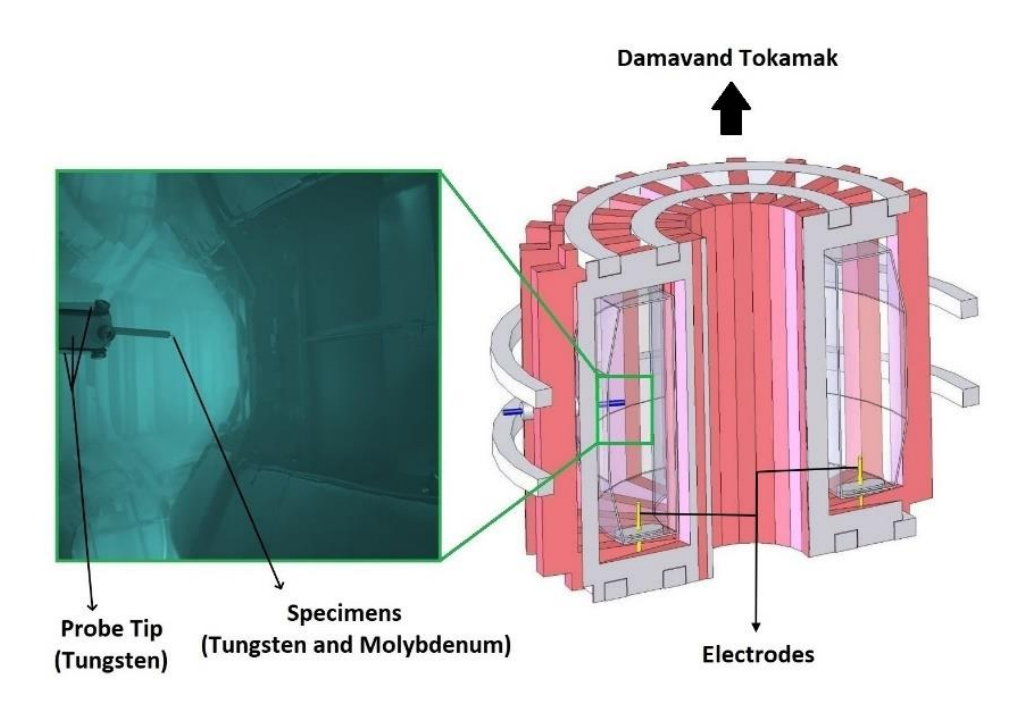


FIG. 1. Schematic view of experimental set-up for He-GDC procedure in Damavand tokamak.

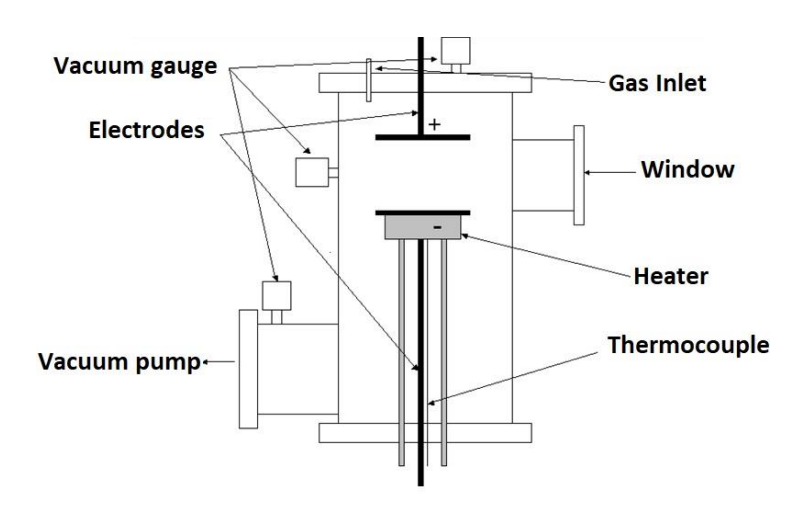


FIG. 2. Schematic view of experimental set-up for He-GDC procedure in a PECVD Device.

A conventional glow discharge procedure using helium gas (purity: 99.9995%) was carried out for three hours. Before the GDC process has been started, the vacuum vessel pressure should be reached to suitable conditions. The vacuum pumping system of Damavand tokamak consisted of two rotary and two turbo molecular pumps, will reach the pressure to appropriate conditions. As illustrated in Fig. 2, first of all, the pressure is fallen down from atmospheric pressure to about 4×10^{-2} Torr by the rotary pumps. Then the turbo molecular pumps come into action and reduce the pressure to about 2×10^{-6} Torr. After that the helium gas is puffed to the vacuum vessel by

an MV-112 piezoelectric valve. The gas puffing procedure is controlled by a PID controller and the pressure could be adjusted to any desired value. Fig. 3 shows the controlled pressure by the gas puffing procedure. When the pressure reaches the determined value, the voltage is applied to the electrodes inserted into the vacuum vessel and the Helium glow discharge plasma is sustained. During the glow discharge plasma regime the pressure was controlled to 2.5×10^{-3} Torr. It should be noted that the discharge parameters were 450 VDC and 1.5A and the temperature of the samples during this procedure is less than 370K. Finally, when the helium gas puffing is accomplished, the species inside the vacuum vessel is pumped out by the pumping system and the pressure reach to about 1.5×10^{-6} Torr. It should be emphasized that the samples were only exposed to the glow discharge plasma and were never subjected to tokamak shots (i.e., magnetic confinement fusion plasma conditions) or any other operational scenarios.

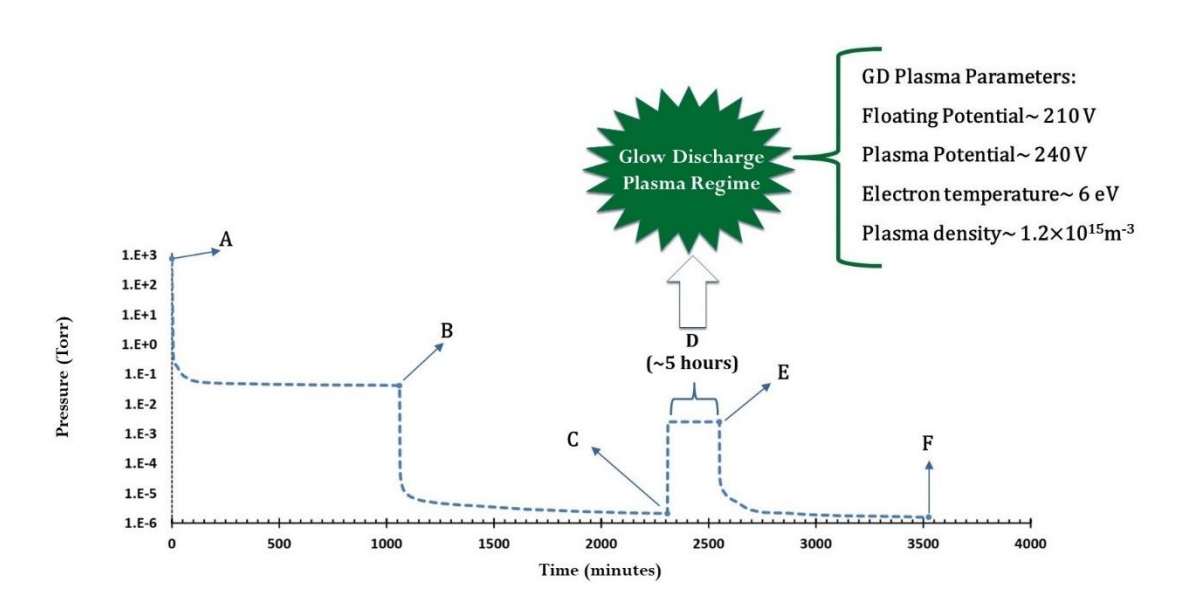


FIG. 3. Time trace diagram of vacuum vessel pressure for a routine He-GDC in Damavand tokamak. A) The rotary pumps start to work. B) The turbo molecular pumps start to work. C) The helium gas is puffed into the vacuum vessel. D) Time duration of glow discharge plasma E) Termination of gas puffing process F. Accomplishment of He-GDC procedure

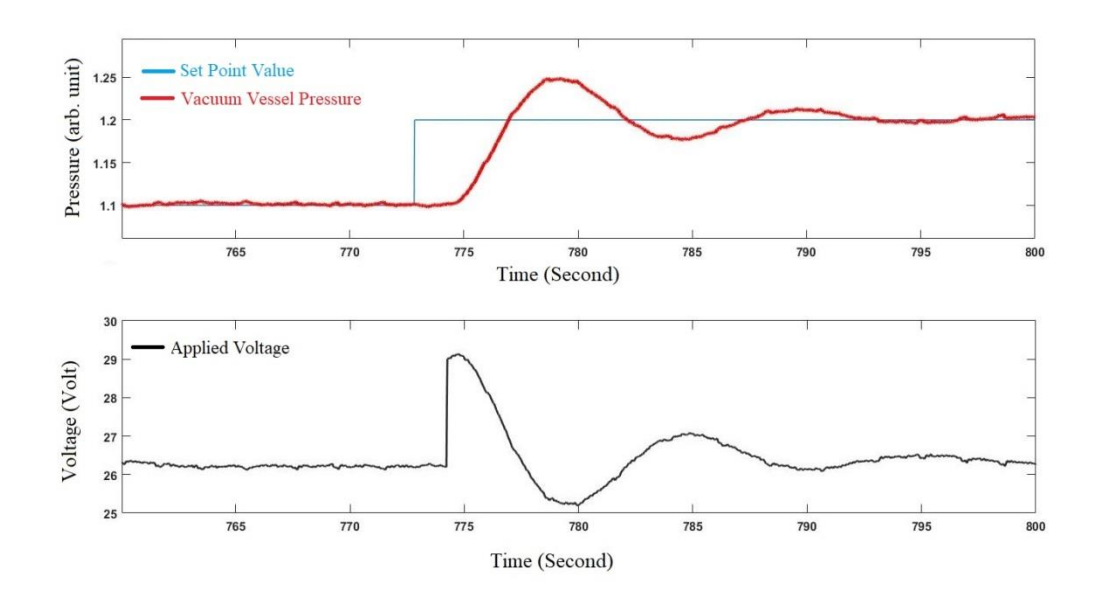


FIG. 2. Adjustment of vacuum vessel pressure in Damavand tokamak by a PID voltage controller applied to piezoelectric valve

3. RESULTS AND DISCUSSION

3-1. Surface Morphology

Several pure W specimens were exposed to He-GD plasma. Fig. 4 shows the SEM images of reference samples that were mechanically polished and not exposed to GDC. As seen, no surface roughness or nanostructures are present. This confirms that the observed post-GDC features result from plasma exposure rather than pre-existing surface conditions.

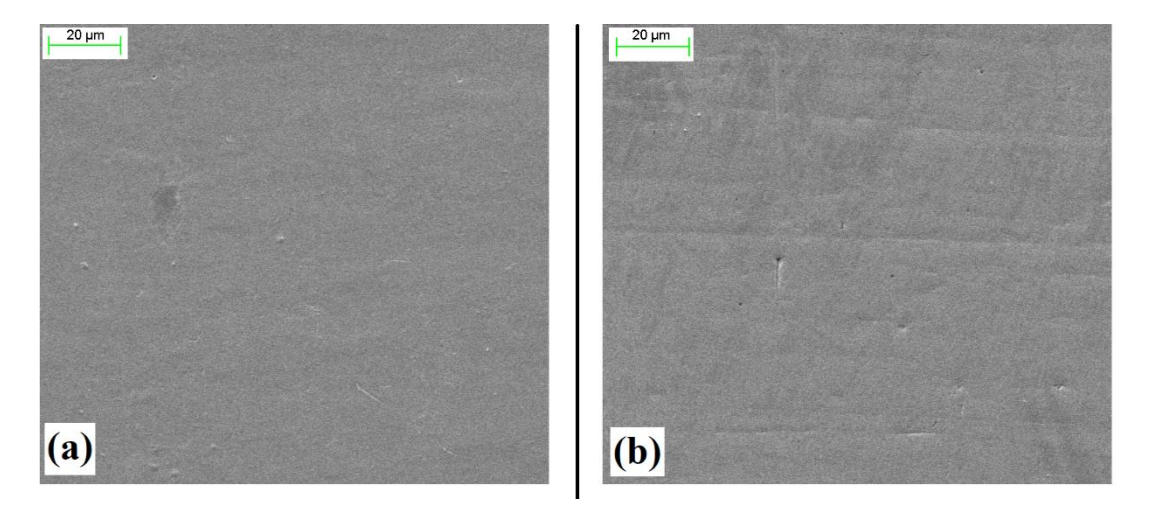


FIG. 3. SEM images of raw (a) tungsten and (b) molybdenum samples that were mechanically polished and not exposed to GD plasma.

Fig. 5 shows SEM images of the W sample. Fuzzy nanostructures are formed in some parts of the surface. These nanostructures do not uniformly cover the surface and are like isolated islands. For a better understanding, a 75° tilted images shown in Fig. 5c, have also been recorded. The area of these islands is about a few tens of square micrometers. Inside these islands, a large number of rods are observed that are formed together in a special order. The size of each of these rods is approximately between 20 and 40 nanometers. Using Energy Dispersive X-Ray analysis (EDX), elemental analysis of these nanostructures was determined. As Fig. 6 shows, these nanostructures are composed of tungsten elements. In fact, EDX analysis shows that the atomic composition of these nanostructures is not different from the reference sample, as well as where these nanostructures have not grown, which suggests that these nanostructures may have created by an intrinsic effect rather than an extrinsic effect.

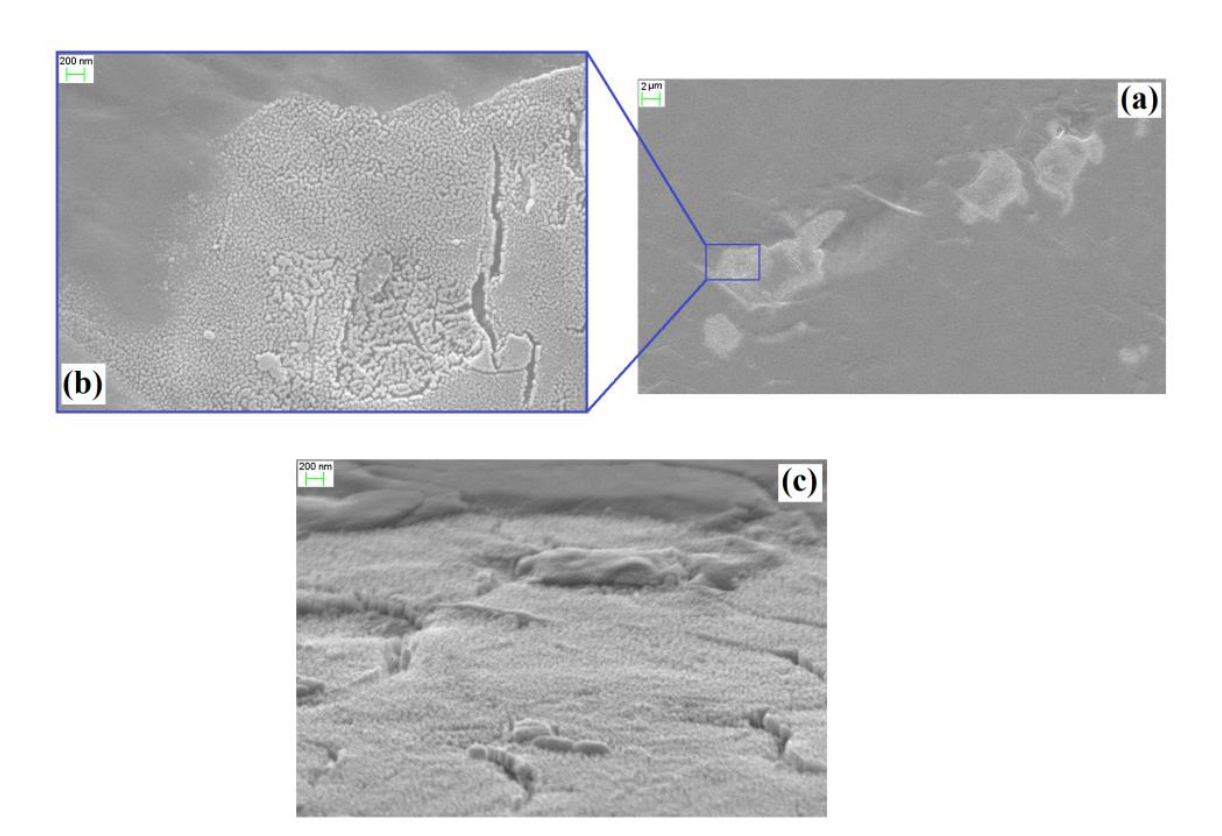


FIG. 5. (a) SEM image of tungsten surface exposed by helium glow discharge plasma (b) high-resolution image of the region (c) tilted image of the region

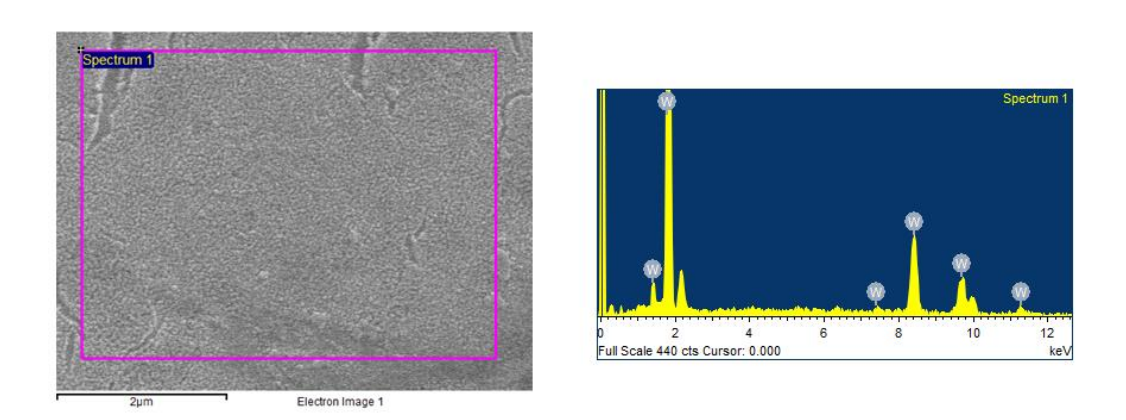


FIG. 4. EDX analysis nanostructures formed on W surface

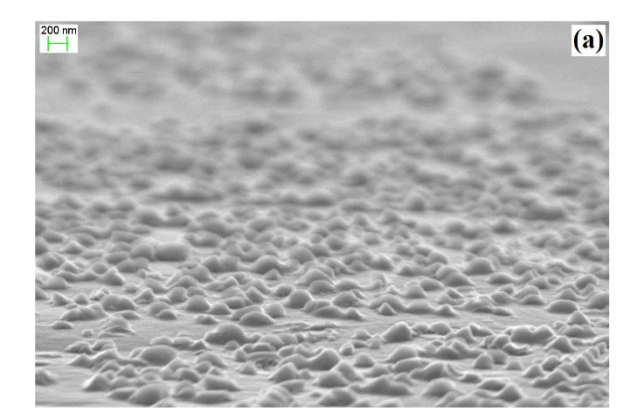
3-2. Impurity Effects and Formation of Isolated Fuzzy Nanostructures

The fuzzy nanostructures have been observed for more than a decade [23]. During this time, the mechanism of the formation process of the fuzz has been extensively investigated. However, this phenomenon is not yet fully understood and there are still several open questions about the cause of formation and growth of these fiber form nanostructures. By reviewing the reports, formation of the fuzz could be occurred under two main following conditions: impact of ion energy modulation, and impact of impurities.

Woller et al. have reported the impact of radiofrequency (RF) modulation of plasma on the formation of fuzzy nanostructures[24]. They observed the nanostructures are formed by RF plasma in the range of 30-100 eV. In their experiments, the formation of nanostructures has also reported even without utilizing RF modulated biasing, and it was deduced that ion energy distribution width of about 70 eV is required for the formation and

growth of fuzz. The impact of impurities on the formation of fuzzy nanostructures has also been reported by Hwangbo et al. as well as Al-Ajlony et al[25, 26]. They observed fuzzy nanostructures by adding impurities such as nitrogen, argon, neon, carbon gases and residual air to Helium plasma. It is interesting to note that a change in gas impurity type and also a subtle change in impurity percentage amount could led to significant morphology changes of nanostructures.

According to the above mentioned conditions and since the plasma produced in Damavand tokamak is a DC plasma, the formation of nanostructures in our experiments is not due to the ion energy distribution and is probably related to the impact of impurities. It should be noted that the experiments conducted in Damayand tokamak leading to the observation of fuzzy nanostructures is a He-GDC process, which is a conventional procedure of wall conditioning in tokamaks. It is normal that before the GDC process, there are some amounts of residual air which is absorbed into the tokamak wall. Hence, by carrying out the GDC, the absorbed atoms can enter to the vacuum vessel and increase the amounts of impurities. Several mechanisms have been so far proposed on how fuzzy nanostructures are formed and grown. The most well-known mechanisms are: 1. Bubble growth and rupture [27], 2. Dislocation and grain boundary segregation [28], 3. Viscoelastic and voidcoalescence models [29], 4. Electric-field induction [30], and 5. Sputtering and erosion [31]. Each of these mechanisms tries to justify how the fuzz phenomenon takes place. Among these mechanisms the explanation based on bubble growth and rupture mechanism is more popular [16]. According to this explanation, the helium atoms firstly implant on the tungsten surface. The single implanted atoms diffuse until they encounter other helium atoms, forming helium clusters. One of the effective factors in formation and growth of fuzzy nanostructures is the fluence. Lasa et al. in [32] performed molecular dynamics simulations of formation and growth of fuzz. According to their results, as the fluence increases, the probability of formation of fuzz also increases. When fluence is too low, the helium atom goes into single interstitial locations. On the other hand, when fluence increases the helium migration process starts and after that, the bubbles are formed by helium atoms. Consequently, the bubbles formed create a pressure leading to growth of fuzz. Due to this point, the experiments in Damavand tokamak were conducted for two different fluences. Fig. 7 shows the tungsten surfaces exposed to He-GDC in low (5.5×1021m-2) and high fluence (2×1022m-2). As Fig. 7a shows, firstly the bubbles are formed by helium atoms. By increasing the exposure time, which subsequently causes the fluence to rise, the fuzzy nanostructures starts to form and growth. Figure 7b shows the exposed tungsten surface at higher fluence. These images validate the molecular dynamics simulation results performed by Lasa et al. indicating the fluence has an important role in growth of fuzzy nanostructure.



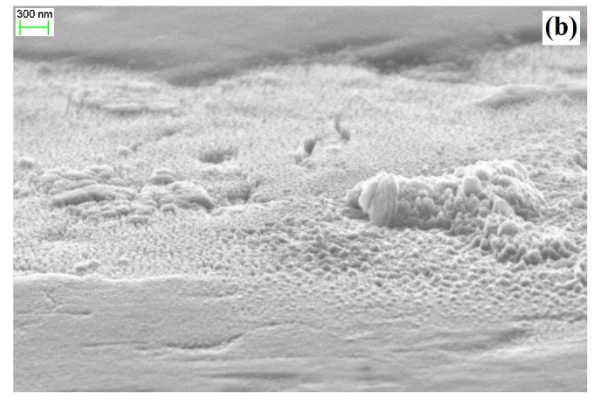


FIG. 5. SEM images of fuzzy nanostructures formed on tungsten surface exposed to (a) low $(5.5 \times 10^{21} \text{m}^{-2})$ and (b) high $(2 \times 10^{22} \text{m}^{-2})$ fluence

3-3. XRD Analysis and Lattice Stress Evolution

X-ray diffraction (XRD) was performed on the specimens to investigate the change in the crystallographic structure of W due to the interaction with He glow discharge plasma. The XRD spectra are shown in Fig. 7. The change in XRD pattern reveals the details of structural variations due to exposure. In the pristine tungsten sample, both plane peaks of $(2\ 0\ 0)$ and $(2\ 1\ 1)$ indicate the body-centered cubic (BCC) phase [33]. There is no new plane in the exposed samples diffraction pattern indicating that plasma exposure did not make any structural phase transformation. There are small shifts detected in the 2θ position of the diffraction peaks after irradiation. In XRD diffractogram, this type of shift can be caused for several reasons, but most notably it can be

a result of a compressive stress on the crystal structure [34]. The helium bubbles accumulations in the crystal structure and grain boundaries essentially push the lattice atoms closer together. Indeed, during the formation of helium bubbles, the tungsten atoms surrounding the bubbles are pushed out, and as figure 7 shows, with increasing the exposure time, the amount of shift in XRD peaks also increases.

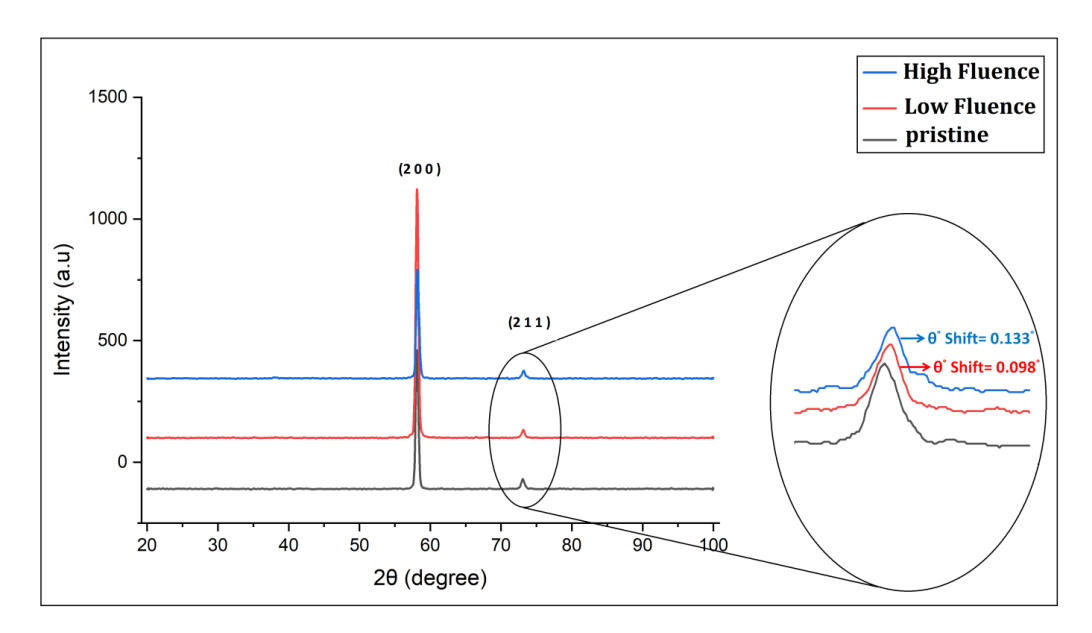


FIG. 6. XRD spectra of pristine W specimen (black) compared to specimens exposed to low (red) and high (blue) fluence helium ions.

According to the mechanism presented for the formation of fuzzy nanostructure [28], the helium bubble formed on the tungsten surface, leaves a hole in the W cell, which somewhat recrystallizes after the helium desorption. The hole left in the W matrix will refill more easily and the helium bubbles formed in these holes will more easily rupture. Therefore, it is expected that the crystallite size will increase due to the formation of bubbles. From diffraction pattern the crystallite size could be calculated using the Debye–Scherrer equation. The following equation, known as Scherrer equation, is used to find the average crystallite size, where D is the crystalline size, K represents the Scherrer constant that is normally taken as 0.94, and λ , θ , and β denote the wavelength, the Braggs angles in radians, and the full width at half maximum (FWHM) of the peak in radians, respectively[35].

$$D = \frac{k\lambda}{\beta\cos\theta} \tag{1}$$

Applying Bragg's law, the interplanar spacing commonly indicated as d_{hkl} can be calculated using the equation $d_{hkl} = \frac{n\lambda}{2\sin\theta}$. Where, n, λ , and θ are Bragg diffraction order, X-ray wavelength, and Bragg angle, respectively[34].using the formula for the (2 1 1) planes, the d-spacing can be calculated. Table 1 shows the values of the parameters for different specimens. According to the Table 1 data, the crystallite size is increased when the fuzzy nanostructures are formed. The growth in lattice parameter size denotes it takes a greater fluence of helium ions hitting the tungsten surface to reach some saturation point at which the fuzz formation processes could continue normally as seen with traditional W samples. Thus, the results of XRD analysis are in good agreement with the bubble growth and rupture mechanism [16].

TABLE 1. XRD ANALYSIS OF TUNGSTEN SAMPLES

Miller index	2θ (degree)			d-spacing (Å)			crystallite size (nm)		
	Pristine	Lower	Higher	Pristine	Lower	Higher	Pristine	Lower	Higher
		fluence	fluence		fluence	fluence		fluence	fluence
2 1 1	73.066	73.164	73.198	1.294	1.293	1.292	19.6	19.6	23.9

3-4. Impact of Floating Potential

The material probe installed in Damavand tokamak has the ability to place the specimens in two different potentials relative to the plasma. The specimens could be placed at ground potential and considered as part of the wall, or they could be placed at floating potential. It is worth noting that generally, the floating voltage (along with other factors) varies during GDC due to changes in impurity levels and wall conditions. The measured variation in floating voltage was within a ~20 V range, which remained relatively stable due to the use of a pressure feedback control system that maintained the discharge pressure at 2.5×10⁻³ Torr. In this study the specimens were examined in both conditions. As it is shown in Fig. 9, an interesting morphology change was detected when the samples were in floating potential. A tilted-view images shown in Fig. 10, have also been recorded to give a better understanding of the morphology change. This morphology changes are so similar to the results recorded by Corr et al.[36]. In the early years, based on the experimental results, the necessary temperature for the formation of the fuzz was reported in the range 1000-2000K [37]. Woller et al. observed this phenomenon at temperatures lower than necessary temperature (870-1220K) [24]. Several years later, Corr et al observed the formation of fuzzy nanostructures at 470K [36]. So the results achieved in the experiment performed in Damavand tokamak also confirm the observation of fuzz phenomenon at low temperatures reported by Corr et al.[36]. It should be noted that in the series of experiments performed in Damavand tokamak, 3 types of specimens have been investigated. In addition to tungsten and molybdenum, which are the important plasma facing components, the stainless steel 316 (SS 316L) has also been examined. Unlike the tungsten and molybdenum samples, the GDC procedure results have been favorable for exposed stainless steel samples. There is no trace of microscopic damage or formation of fuzzy nanostructures in stainless steel specimens. Anyway, observing the favorable results for stainless steel specimens was predictable, because Damavand tokamak chamber (such as many other tokamaks) is made of stainless steel and GDC technique which is its main wall conditioning procedure, has been utilized for many years. Altogether, the results show that He-GDC procedure, contrary to the beneficial effects on stainless steel, cannot be so useful and favorable for refractory plasma facing materials such as tungsten and molybdenum.

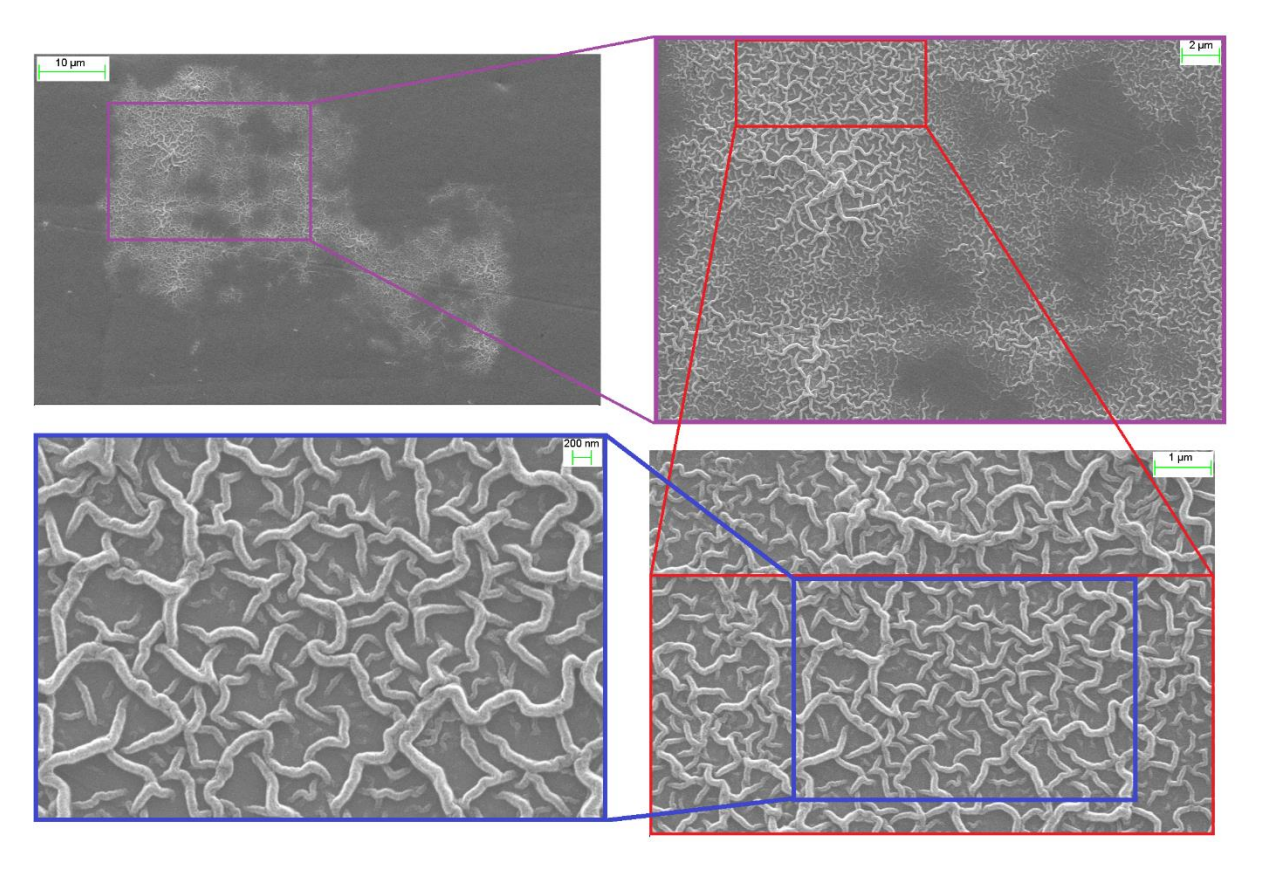


FIG. 7. Morphology change in Molybdenum specimens.

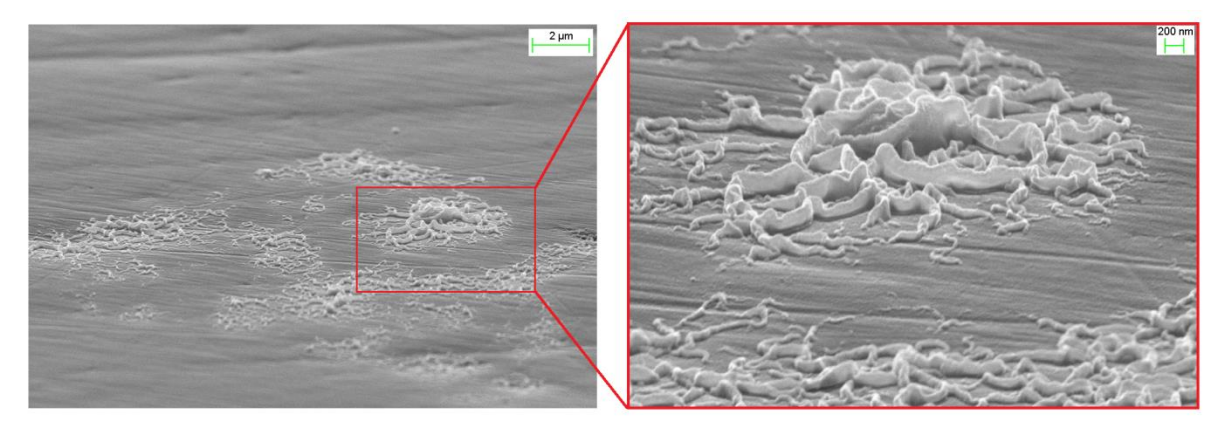


FIG. 8. Tilted view of morphology change in Molybdenum specimens.

3-5. Observing Similar Results Using a PECVD Device

In addition to the tokamak device, a DC glow discharge plasma device (a PECVD device) was also used. In fact, plasma devices may provide a reliable platform for investigating the impact of plasma ions on surfaces, simulating conditions relevant to tokamak environments. Additionally, Plasma-Enhanced Chemical Vapor Deposition (PECVD) techniques offer precise control over plasma exposure, allowing researchers to analyze the evolution of surface features at different plasma conditions such as glow discharge cleaning environments. By employing these methods, it is possible to gain deeper insights into the mechanisms responsible for tungsten surface modification in helium-rich plasmas.

As Figure 10 shows, the fibre-like nano-structures are formed on the surface of tungsten specimens. The fuzzy nanostructures didn't cover the surface completely and were grown as the isolated islands. Reports published to date suggest that isolated fuzzy nanostructures develop under two key conditions: the influence of ion energy modulation[22, 24] and the presence of impurities[25, 26, 38]. Since a dc plasma was used in these experiments, the formation of these nanostructures cannot be due to ion energy modulation and is probably due to the presence of impurities. It should be noted that since the vacuum vessel of the PECVD device must be opened for specimen mounting, and the base pressure in the experiments is approximately 2×10^{-2} Torr, it is normal for small amounts of residual air to mix with the helium plasma. Furthermore, in ITER and DEMO, impurity gas seeding is considered a key method for heat-load mitigation to protect divertor plates during standard operation campaigns[39, 40]. Therefore, it is crucial to investigate the potential effects of impurity ion irradiation on the morphological changes of the tungsten surface.

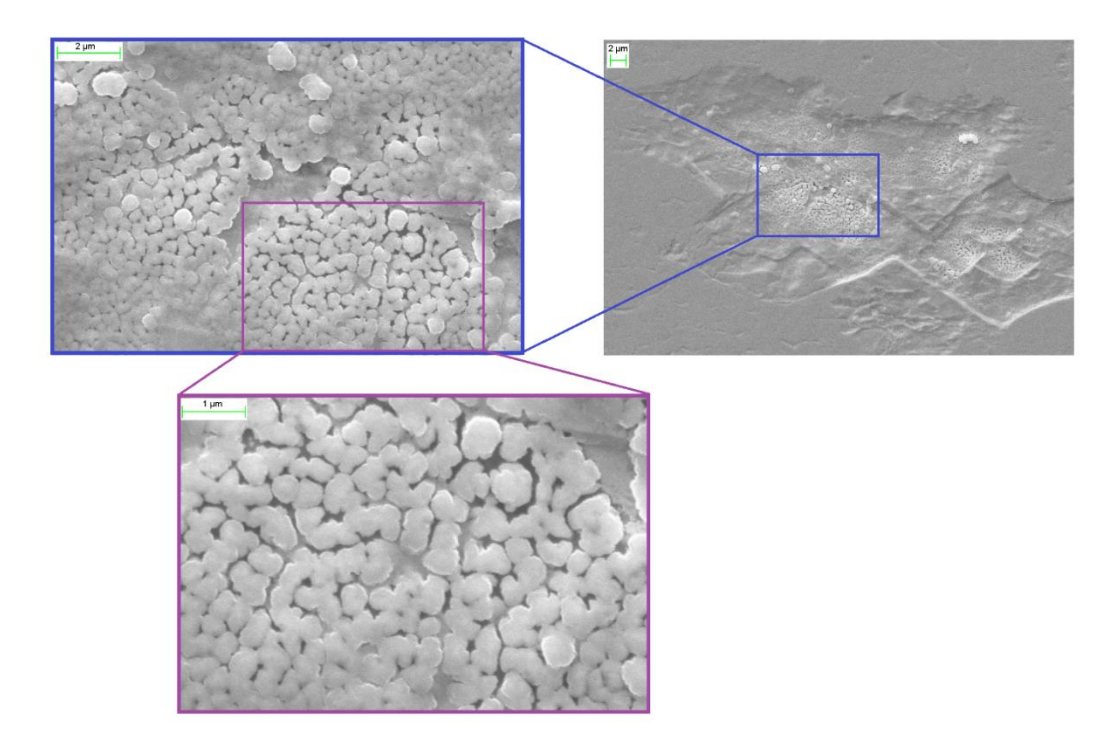


FIG. 10.SEM image of tungsten surface exposed by helium glow discharge plasma in different magnifications

To better understand the formation of these nanostructures, SEM images were also captured at a 75-degree tilt angle. As illustrated in Figure 11, there are fiber-like nanostructures within the islands, each covering an area of tens of square micrometers. The width of nanorods inside the island varies from 200 nm to 700 nm. Energy Dispersive X-Ray Analysis (EDX) was used to determine the elemental composition of these nanostructures. It indicated that these nanostructures consist of tungsten. Notably, EDX analysis reveals that their atomic composition is similar to that of the reference sample and to regions where these nanostructures have not formed. This implies that their formation is likely driven by an intrinsic effect rather than an extrinsic one.

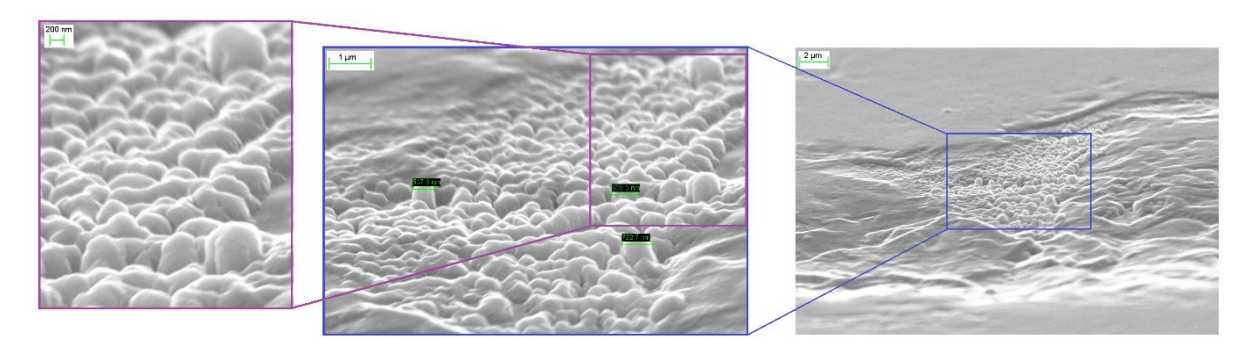


FIG. 11. Tilted-view SEM image of tungsten surface exposed by helium glow discharge plasma in different magnifications.

Using EDS analysis line scan, some important information was revealed. As illustrated in Figure 12, oxygen atoms accumulate more in the regions where the fuzzy nanostructures exist. Based on the previous reports, oxygen atoms are capable of trapping helium atoms in tungsten [41-43]. Oxygen exhibits a much larger binding energy with helium compared to other interstitial solutes. This means that helium atoms are more strongly attracted to and retained around oxygen atoms. Because of this strong attraction, oxygen impurities can act as helium trapping centers, leading to a local increase in helium concentration around oxygen atoms. Since helium accumulation is a key factor in fuzz formation, controlling the oxygen content in tungsten is important to regulate helium behavior and potentially influence fuzz growth. In conclusion, oxygen atoms significantly enhance helium trapping in tungsten, making their concentration a crucial factor in managing helium retention and its effects on material properties.

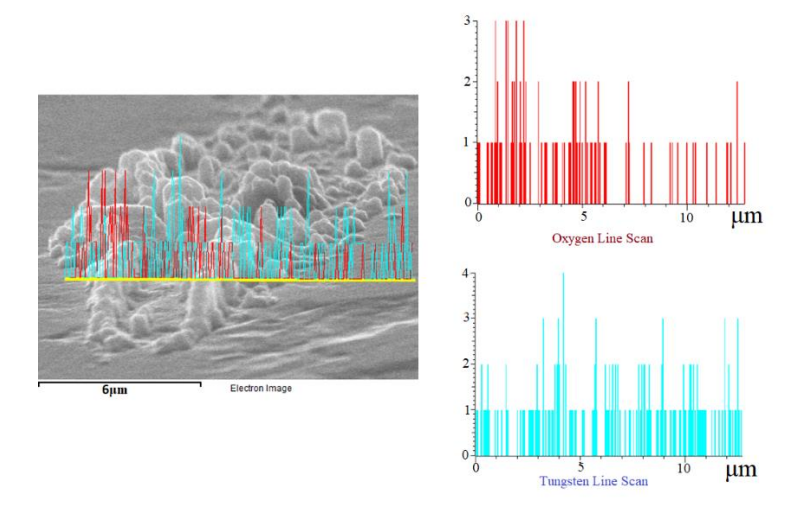


FIG. 12. SEM micrograph and EDS analysis line scan results for oxygen and tungsten elements.

4. CONCLUSION

Observation of fuzz phenomenon in recent years has caused the interaction of low energy helium ions with tungsten to become a new and significant challenge for the construction of fusion reactors. These fuzzy and loose nanostructures can be easily detached from the tungsten surface and act as a source of dust particles and impurities and consequently cool the plasma. Due to the importance of this issue, considerable experimental investigations and simulations have been started to reveal its various features. Although the early studies indicated that they generally form under certain conditions in terms of surface temperature, ion incident energy, and ion fluence, the recent experimental results have shown that they can also form at lower temperatures and outside these conditions. Although much significant research has been done so far, the mechanism of fuzz has yet to be fully understood and further experimental investigations definitely can lead to a better understanding. This study provides direct experimental evidence of growth of fuzzy nanostructures on the surface of tungsten and molybdenum resulting from helium glow discharge cleaning (He-GDC) in an operational tokamak environment. The formation of isolated fuzzy nanostructures appears to be strongly influenced by impurity effects rather than ion energy distribution alone, consistent with previous reports. Although in-situ impurity analysis was not available, the use of high-purity helium gas and the stable vacuum conditions suggest that residual wall-adsorbed species may have contributed to nanostructure growth. Fluence dependence played a critical role, with higher fluences correlating with more pronounced fuzz formation. This supports simulationbased models that link helium implantation and bubble evolution to nanostructure growth mechanisms. X-ray diffraction (XRD) analysis revealed lattice distortion in the form of peak shifts, without new phase formation. These shifts are attributed to compressive stress induced by helium bubble accumulation, and increased crystallite size was observed at higher fluences.

The helium glow discharge cleaning procedure, one of the primary methods for vacuum vessel conditioning in fusion devices, is widely used in current tokamaks and is planned for future reactors such as ITER. In this study, microscopic modifications of major plasma-facing materials—tungsten and molybdenum—interacted with helium ions in a GDC regime have been investigated in the Damavand tokamak and a PECVD device. Our findings are the first direct evidence of the formation and growth of fiber-like nanostructures similar to tungsten fuzz on these materials following routine GDC operation. These observations suggest that while GDC is crucial for wall conditioning, it may also introduce microscopic damage in tungsten/molybdenum regions such as divertors. Caution is advised in its use under such conditions.

REFERENCES

- [1] S. Sridhar *et al.*, "Characterization of cold background plasma during the runaway electron beam mitigation experiments in the JET tokamak," *Nuclear Fusion*, vol. 60, no. 9, p. 096010, 2020.
- [2] J. Wesson and D. J. Campbell, *Tokamaks*. OUP Oxford, 2011.
- [3] M. Shimada, S. Putvinski, and R. A. Pitts, "Glow discharge cleaning on ITER," *38th EPS Conference on Plasma Physics 2011, EPS 2011 Europhysics Conference Abstracts*, vol. 35, pp. 1564-1567, 01/01 2011.
- [4] Z. Khan *et al.*, "Conditioning of SST-1 Tokamak Vacuum Vessel by Baking and Glow Discharge Cleaning," *Fusion Engineering and Design*, vol. 103, pp. 69-73, 2016.
- [5] Y. Yamauchi, K. Takeda, Y. Nobuta, and T. Hino, "Hydrogen and helium removal retained in stainless steel by neon glow discharge," *Journal of Nuclear Materials*, vol. 390, pp. 1048-1050, 2009.
- [6] M. Shimada and R. A. Pitts, "Wall conditioning on ITER," *Journal of Nuclear Materials*, vol. 415, no. 1, Supplement, pp. S1013-S1016, 2011/08/01/2011.
- [7] G. J. M. Hagelaar, D. Kogut, D. Douai, and R. A. Pitts, "Modelling of tokamak glow discharge cleaning I: physical principles," *Plasma Physics and Controlled Fusion*, vol. 57, no. 2, p. 025008, 2014/12/22 2014.
- [8] S. Masuzaki *et al.*, "Wall Conditioning in LHD," *Fusion Science and Technology*, vol. 58, no. 1, pp. 297-304, 2010.
- [9] M. Miyamoto *et al.*, "Microscopic damage of materials exposed to glow discharge cleanings in LHD," *Journal of Nuclear Materials*, vol. 329, pp. 742-746, 2004.
- [10] M. Tokitani *et al.*, "Microscopic modification of wall surface by glow discharge cleaning and its impact on vacuum properties of LHD," *Nuclear Fusion*, vol. 45, no. 12, p. 1544, 2005.
- [11] P. Semwal *et al.*, "Baking and helium glow discharge cleaning of SST-1 Tokamak with graphite plasma facing components," *Journal of Physics: Conference Series*, vol. 823, p. 012061, 2017/04/19 2017.
- [12] G. Zhuang *et al.*, "The reconstruction and research progress of the TEXT-U tokamak in China," *Nuclear Fusion*, vol. 51, no. 9, p. 094020, 2011/08/31 2011.
- [13] V. Rohde, R. Dux, A. Kallenbach, K. Krieger, and R. Neu, "Wall conditioning in ASDEX Upgrade," *Journal of Nuclear Materials*, vol. 363-365, pp. 1369-1374, 2007/06/15/ 2007.
- [14] D. Kogut, D. Douai, G. Hagelaar, and R. Pitts, "Modelling the ITER glow discharge plasma," *Journal of Nuclear Materials*, vol. 463, pp. 1113-1116, 2015.
- [15] S. Takamura, N. Ohno, D. Nishijima, and S. Kajita, "Formation of nanostructured tungsten with arborescent shape due to helium plasma irradiation," *Plasma and fusion research*, vol. 1, pp. 051-051, 2006.
- [16] K. D. Hammond, "Helium, hydrogen, and fuzz in plasma-facing materials," *Materials Research Express*, vol. 4, no. 10, p. 104002, 2017/10/05 2017.
- [17] F. Sefta, K. D. Hammond, N. Juslin, and B. D. Wirth, "Tungsten surface evolution by helium bubble nucleation, growth and rupture," *Nuclear Fusion*, vol. 53, no. 7, p. 073015, 2013.
- [18] G. Wright *et al.*, "Tungsten nano-tendril growth in the Alcator C-Mod divertor," *Nuclear Fusion*, vol. 52, no. 4, p. 042003, 2012.
- [19] G. M. Wright *et al.*, "Comparison of tungsten nano-tendrils grown in Alcator C-Mod and linear plasma devices," *Journal of Nuclear Materials*, vol. 438, pp. S84-S89, 2013/07/01/ 2013.
- [20] A. Khan, G. De Temmerman, T. W. Morgan, and M. B. Ward, "Effect of rhenium addition on tungsten fuzz formation in helium plasmas," *Journal of Nuclear Materials*, vol. 474, pp. 99-104, 2016/06/01/2016.
- [21] Y. Ueda *et al.*, "Exposure of tungsten nano-structure to TEXTOR edge plasma," *Journal of Nuclear Materials*, vol. 415, no. 1, Supplement, pp. S92-S95, 2011/08/01/2011.
- [22] K. B. Woller, D. G. Whyte, and G. M. Wright, "Isolated nano-tendril bundles on tungsten surfaces exposed to radiofrequency helium plasma," *Nuclear Materials and Energy*, vol. 12, pp. 1282-1287, 2017/08/01/2017.
- [23] S. Takamura, N. Ohno, D. Nishijima, and S. Kajita, "Formation of nanostructured tungsten with arborescent shape due to helium plasma irradiation," *Plasma Fusion Research*, vol. 1, pp. 051-051, 2006.
- [24] K. Woller, D. Whyte, and G. Wright, "Impact of helium ion energy modulation on tungsten surface morphology and nano-tendril growth," *Nuclear Fusion*, vol. 57, no. 6, p. 066005, 2017.
- [25] D. Hwangbo, S. Kajita, N. Ohno, P. McCarthy, J. W. Bradley, and H. Tanaka, "Growth of nano-tendril bundles on tungsten with impurity-rich He plasmas," *Nuclear Fusion*, 2018.

- [26] A. Al-Ajlony, J. Tripathi, and A. Hassanein, "Role of carbon impurities on the surface morphology evolution of tungsten under high dose helium ion irradiation," *Journal of Nuclear Materials*, vol. 466, pp. 569-575, 2015.
- [27] A. Lasa, S. Tähtinen, and K. Nordlund, "Loop punching and bubble rupture causing surface roughening—a model for W fuzz growth," *EPL (Europhysics Letters)*, vol. 105, no. 2, p. 25002, 2014.
- [28] E. Martínez, B. P. Uberuaga, and B. D. Wirth, "Atomistic modeling of helium segregation to grain boundaries in tungsten and its effect on de-cohesion," *Nuclear Fusion*, vol. 57, no. 8, p. 086044, 2017.
- [29] S. Krasheninnikov, "Viscoelastic model of tungsten 'fuzz' growth," *Physica Scripta*, vol. 2011, no. T145, p. 014040, 2011.
- [30] K. B. Woller, D. G. Whyte, G. M. Wright, and D. Brunner, "Experimental investigation on the effect of surface electric field in the growth of tungsten nano-tendril morphology due to low energy helium irradiation," *Journal of Nuclear Materials*, vol. 481, pp. 111-116, 2016.
- [31] R. P. Doerner, M. J. Baldwin, and P. C. Stangeby, "An equilibrium model for tungsten fuzz in an eroding plasma environment," *Nuclear Fusion*, vol. 51, no. 4, p. 043001, 2011.
- [32] A. Lasa, K. O. E. Henriksson, and K. Nordlund, "MD simulations of onset of tungsten fuzz formation under helium irradiation," *Nuclear Instruments and Methods in Physics Research Section B: Beam Interactions with Materials and Atoms*, vol. 303, pp. 156-161, 2013/05/15/2013.
- [33] Y. Ueda *et al.*, "Research status and issues of tungsten plasma facing materials for ITER and beyond," *Fusion Engineering and Design*, vol. 89, no. 7, pp. 901-906, 2014/10/01/2014.
- [34] S. Gonderman, J. K. Tripathi, T. J. Novakowski, T. Sizyuk, and A. Hassanein, "The effect of low energy helium ion irradiation on tungsten-tantalum (W-Ta) alloys under fusion relevant conditions," *Journal of Nuclear Materials*, vol. 491, pp. 199-205, 2017/08/01/2017.
- [35] F. Sedighi *et al.*, "Investigation of hydrogen glow discharge cleaning side effects on tungsten," *Plasma Physics Reports*, vol. 47, pp. 128-138, 2021.
- [36] C. S. Corr *et al.*, "Mechanical properties of tungsten following rhenium ion and helium plasma exposure," *Nuclear Materials and Energy*, vol. 12, pp. 1336-1341, 2017/08/01/ 2017.
- [37] S. Kajita, W. Sakaguchi, N. Ohno, N. Yoshida, and T. Saeki, "Formation process of tungsten nanostructure by the exposure to helium plasma under fusion relevant plasma conditions," *Nuclear Fusion*, vol. 49, no. 9, p. 095005, 2009.
- [38] D. Hwangbo, S. Kajita, H. Tanaka, and N. Ohno, "Growth process of nano-tendril bundles with sputtered tungsten," *Nuclear Materials and Energy*, vol. 18, pp. 250-257, 2019/01/01/ 2019.
- [39] G. W. Pacher, H. D. Pacher, G. Janeschitz, A. S. Kukushkin, V. Kotov, and D. Reiter, "Modelling of DEMO core plasma consistent with SOL/divertor simulations for long-pulse scenarios with impurity seeding," *Nuclear fusion*, vol. 47, no. 5, p. 469, 2007.
- [40] R. Wenninger *et al.*, "Advances in the physics basis for the European DEMO design," *Nuclear Fusion*, vol. 55, no. 6, p. 063003, 2015.
- [41] C. S. Becquart, M. F. Barthe, and A. De Backer, "Modelling radiation damage and He production in tungsten," *Physica scripta*, vol. 2011, no. T145, p. 014048, 2011.
- [42] C. S. Becquart and C. Domain, "Solute–point defect interactions in bcc systems: Focus on first principles modelling in W and RPV steels," *Current Opinion in Solid State and Materials Science*, vol. 16, no. 3, pp. 115-125, 2012/06/01/2012.
- [43] X. Wu *et al.*, "Effects of alloying and transmutation impurities on stability and mobility of helium in tungsten under a fusion environment," *Nuclear Fusion*, vol. 53, no. 7, p. 073049, 2013.